Chemical Physics 166 (1992) 287–297
North-Holland

The structure of different phases of pure C_{70} crystals

M.A. Verheijen, H. Meekes, G. Meijer, P. Bennema
Research Institute for Materials, Faculty of Science, University of Nijmegen, Toernooiveld, 6525 ED Nijmegen, The Netherlands

J.L. de Boer, S. van Smaalen
Laboratory of Chemical Physics, University of Groningen, Nijenborgh 4, 9747 AG Groningen, The Netherlands

G. van Tendeloo, S. Amelinckx, S. Muto and J. van Landuyt
University of Antwerp (RUCA), Groenenborgerlaan 171, B-2020 Antwerp, Belgium

Received 1 June 1992

Single crystals of pure C_{70} are grown from the vapour phase and the structure and morphology of these crystals is studied. By means of X-ray diffraction and TEM measurements five different phases are observed. The observed phases are (from high to low temperatures) fcc, rhombohedral, ideal hcp ($c/a=1.63$), deformed hcp ($c/a=1.82$) and a monoclinic phase. The occurrence of these different phases and the phase transitions is accounted for in a simple model. For the monoclinic structure a model for the stacking of the orientationally ordered molecules in the lattice is proposed. For both the hcp and fcc phases a Lennard-Jones type interaction potential is used to calculate bond strengths, lattice energies and the theoretical morphology.

1. Introduction

Since the discovery of a method to synthesize fullerenes in macroscopic amounts [1] a lot of research has been performed on especially C_{60}. Several groups have succeeded in growing pure, monocrystalline C_{60} crystals with sizes of some tenths of a mm and various techniques have been applied to determine the crystal structures of the different phases. Above 250 K the molecules form a fcc lattice, in which they have complete rotational freedom. Below 260 K the crystal structure becomes simple cubic with four molecules per unit cell. The C_{60} molecules are still at the same relative positions as in the high temperature phase, but the four positions per cell have become inequivalent due to rotational ordering [2,3]. At lower temperatures the structure becomes fcc again with doubled cell parameters [4].

Correspondence to: M.A. Verheijen, Research Institute for Materials, Faculty of Science, University of Nijmegen, Toernooiveld, 6525 ED Nijmegen, The Netherlands.

About the crystalline form of C_{70}, however, very little is known. Thus far, only results on powder samples have been reported. Vaughan et al. [5] describe the high temperature structure of crystalline powder grown from the vapour phase as being a mixture of hcp ($a=10.62$ Å, $c=17.31$ Å) and fcc ($a=15.01$ Å) and report on two reproducible phase transitions with onsets at 276 and 337 K.

We succeeded in growing large, pure crystals of C_{70} from the vapour phase and we here report on five different phases as determined by X-ray diffraction and TEM measurements. The observed phases are (from high to low temperatures) fcc, rhombohedral, ideal hcp ($c/a=1.63$), deformed hcp ($c/a=1.82$) and a monoclinic phase. The occurrence of and relations between the five phases is discussed. For the monoclinic structure a model for the stacking of the orientationally ordered molecules in the lattice is proposed. For both hcp phases and for the fcc phase a Lennard-Jones type potential is used to describe the interaction between the molecules in the lattice and to estimate the lattice energies. With this potential we are able to predict the equilibrium morphology of

the crystals which is compared to the experimentally observed morphology.

2. Crystal growth

The C_{70} crystals used in this study are grown in a similar way as C_{60} crystals [6]. Carbon soot is produced in a dc arc discharge between two high purity graphite electrodes in a 0.2 atm He environment [1]. Extraction of this soot in cold toluene is used to separate (mainly) C_{60} and C_{70} from the rest. Repeated liquid column chromatography is used to obtain C_{70} with a purity of at least 99.9% [#1]. About 5–10 mg of this C_{70} material is placed at the closed end of a 50 cm long, 1 cm diameter quartz tube with four necks at equal distances. The tube is evacuated down to 10^{-5} Torr and heated to 250°C for several hours to remove all the solvent from the C_{70} powder.

During all further heat treatments the quartz tube is kept at low pressure by continuous pumping. The end of the tube that contains the C_{70} powder is placed in a furnace and heated up to 700°C. The vapour pressure of C_{70} is strongly dependent on the temperature and the sublimed C_{70} solidifies in the next section of the quartz tube, which is kept at some 550–600°C. Thus a large part of the C_{70} is vapour transported between two sections in approximately half an hour. Only a very small fraction of the powder stays behind in the first section. We then melt off this segment and repeat the vapour transport two more times. Almost all of the material can easily be vapour transported into the fourth segment, which is subsequently sealed of on both sides.

The isolated C_{70} is then placed in a furnace kept at 675°C for half an hour and cooled down to room temperature in about 4 hours. C_{70} crystals as large as $0.5 \times 0.5 \times 0.5$ mm^3 are obtained in this way (see fig. 1). Note that the actual growth temperature lies between 675 and 625°C. Most of the crystals have a fcc morphology with {100} and {111} faces, many of them being severely twinned. Some crystals, however, have a hcp morphology with {0001} and $\{10\bar{1}1\}$ faces and maybe also {1000} faces. The presence of the latter faces could not be verified due to the fact that the crystals formed a twin with a fcc part and/or showed only some of the faces because they were attached to the side of the quartz tube. It has to be noted

[#1] Part of the C_{70} material we used (with a stated purity of 99.9% or better) was kindly supplied to us by H. Jonkman (Symcom, The Netherlands).

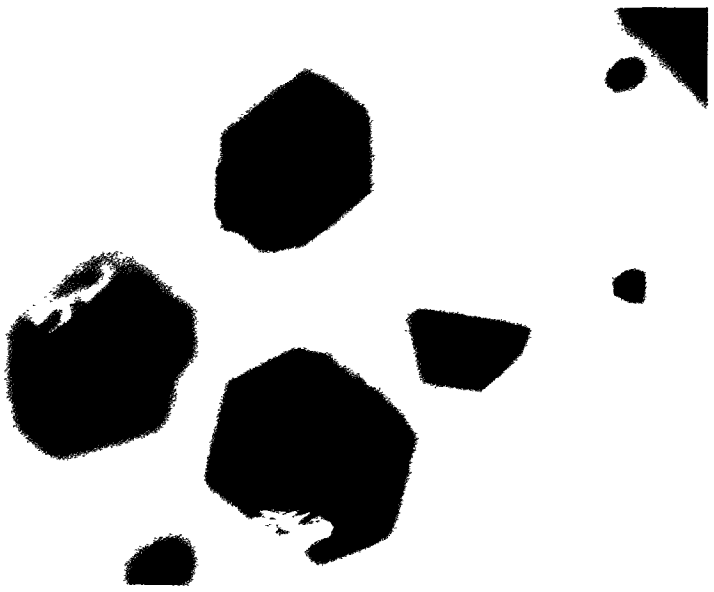

Fig. 1. C_{70} crystals, the lower one having the fcc structure, the upper one having the hcp structure.

that only three out of the approximately 40 crystals grown have the hcp structure. The two types of crystals are grown at the same temperature.

3. The X-ray diffraction measurements

The lattice parameters of the different phases of C_{70} crystals were determined using a four circle diffractometer. The temperature was regulated using a nitrogen gas flow.

Both a fcc and a hcp grown crystal were analysed at room temperature. Although the morphology of the fcc crystal was obvious, the lattice parameters could not be determined due to severe twinning and a possibly disordered structure at low temperatures. Also at higher temperatures neither the fcc nor the rhombohedral phase could be identified; re-heating the crystals in the diffractometer resulted in a very poor crystal quality. A good analysis was therefore not possible.

The X-ray diffraction pattern of the crystals with a hcp morphology could be interpreted more easily. At room temperature two crystal structures were found. First, a hcp structure having the extinction conditions of the space group $P6_3/mmc$. The lattice constants are $a=b=10.56$ Å and $c=17.18$ Å ($Z=2$). The reliability factor for averaging equivalent reflections is $R_I=\sum|I-I_{av}|/\sum I=1.7\%$ indicating the hexagonal symmetry to be present at least in a very good approximation. Only reflections with $I>2.5\sigma_I$, where σ_I is the estimated standard deviation in I, were included in the calculations. The second crystal phase of the hcp grown crystals determined at room temperature has also a hcp structure. The lattice parameters are $a=b=10.11$ Å and $c=18.58$ Å ($Z=2$). The R_I factor is 11.1%. The R_σ value, which gives the average of the relative error in the intensities, is 5.8% indicating a reasonable fit of the data set. For the latter phase also averaging in the lower symmetry space group $P12_1/m1$ was performed resulting in $R_I=5.8\%$ and $R_\sigma=4.1\%$ thus giving a better fit. However, because the extinction conditions are still those of $P6_3/mmc$ we conclude this phase to be hexagonal as well.

Finally, for the hcp grown crystal the low temperature phase was measured at two different temperatures, namely 220 and 100 K. At both temperatures a cell parameter doubling for a and b was found. This resulted in $a=b=20.04$ Å and $c=18.53$ Å ($Z=8$) at 220 K. Again averaging was performed on both a hexagonal symmetry ($R_I=11.8\%$, $R_\sigma=6.7\%$) and a monoclinic symmetry ($R_I=6.4\%$, $R_\sigma=5.3\%$). At 100 K we found $a=c=19.96$ Å and $b=18.51$ Å, $R_I=11.5\%$ (hexagonal) and $R_I=5.4\%$ (monoclinic, $\alpha=\gamma=90°$, $\beta=120°$). The reflection conditions corresponding to $P6_3/mmc$ are lost, also when only the subcell is considered. Regarding these data it can be concluded that the structure is no longer hcp but rather monoclinic having its unique axis along the direction of the former hexagonal axis.

4. The TEM studies

Electron diffraction and electron microscopy studies were also performed on both hcp and fcc grown crystals. Both crystal types were studied in situ in a wide temperature range from liquid nitrogen temperature to above room temperature. In order to minimize deformation during specimen preparation the crystals were crushed at liquid nitrogen temperature.

The fcc grown crystals show the abcabc stacking mode at all temperatures. No transformation into the abab stacking is observed on cooling these samples. The effective c/a ratio is temperature dependent, however. Around room temperature the crystals are rhombohedral, the long diagonal (the threefold axis) being parallel to the [111] direction. As the temperature increases the rhombohedral deformation decreases and the crystal finally becomes fcc having a lattice parameter of $a=14.96$ Å.

The hcp grown crystals show a hexagonal stacking at room temperature. It has to be noted that the prepared specimens of these crystals became predominantly abcabc stacked after keeping them at room temperature for a few days. Cooling these abcabc stacked fragments to liquid nitrogen temperature did not revert the stacking to hexagonal. The transition hexagonal → cubic is thus irreversible; its rate depends, moreover, on the particle size and occurs more rapidly in the finely divided crystalline material than in bulk crystals.

The room temperature diffraction pattern along the $[2\bar{1}\bar{1}0]$ zone taken from a freshly prepared specimen of a hexagonal crystal reveals a c/a ratio of approximately 1.64, which is close to the value for the ideal

hcp structure. It exhibits streaked spots along two out of three c^* rows, the third row being unstreaked. The streaked diffraction spots are slightly shifted along the c^* direction towards the positions of the fcc spots in the corresponding section. This shows that the specimen, although predominantly hexagonal, is heavily faulted.

The high resolution images along a zone parallel to the close packed rows of molecules reveal the stacking directly (fig. 2). It is found that the room temperature structure is a mixture of faulted fcc and hcp stacked bands. Such a microstructure is typical of a specimen which underwent an incomplete shear transformation by the propagation of Shockley partial dislocations along close-packed planes. The image shows that the transformation occurred in the sense abab...→abcabc... since all interfaces of transformed bands are parallel to the same close packed plane namely the (0001) family of planes of the hexagonal phase, which becomes after transformation a (111) family of planes in the abcabc... phase.

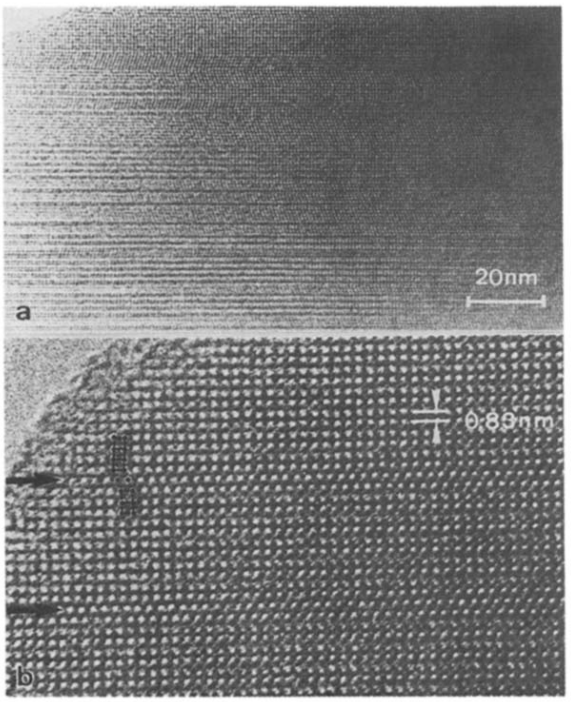

Fig. 2. High resolution image showing the interweaving of fcc and hcp bands. In the high magnification of (b) two stacking faults in the hcp phase are indicated by arrows.

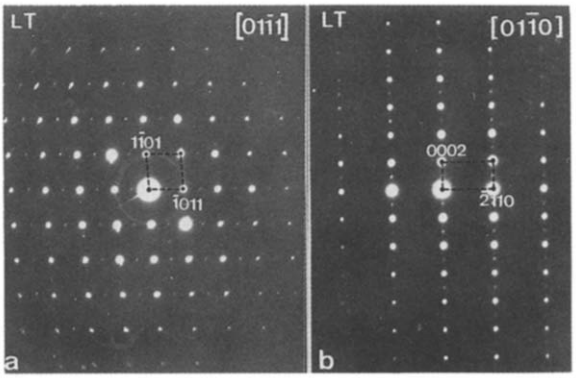

Fig. 3. Low temperature electron diffraction patterns of hcp grown C_{70}. (a) The [01$\bar{1}$1] pseudo-hexagonal section. (b) The [01$\bar{1}$0] pseudo-hexagonal section.

At elevated temperatures also a structure was found having an abcabc stacking. The quantity equivalent to the c/a ratio was found to be slightly above the ideal one, i.e. $c/a \approx 1.66$. It decreases to the ideal one with increasing temperature, resulting in a fcc structure at high temperatures. The corresponding high resolution image leads to very nearly the same c/a ratio showing that the structure is slightly rhombohedral. The [001] image exhibits rows of bright dots which are not mutually perpendicular but enclose an angle of $\approx 91°$.

On cooling a freshly prepared crystal fragment exhibiting a hexagonal diffraction pattern a phase transition from the ideal hcp structure towards the deformed hcp structure is found to occur slightly above room temperature. The c/a ratio increases from 1.64 to 1.82 as has been confirmed by electron diffraction as well as by direct measurement from high resolution images.

On further cooling these samples to liquid nitrogen temperature, superstructure spots develop below around 270 K. In the [01$\bar{1}$0] zone (fig. 3b) the spots with l=odd, which are normally extinct become visible and in the [10$\bar{1}$1] zone of fig. 3a weak supplementary spots appear along the [10$\bar{1}$1]* rows of reflections, midway between the basic spots. The c/a ratio is now ≈ 1.83.

5. Discussion of the different phases

In fig. 4 a phase diagram is shown, indicating the

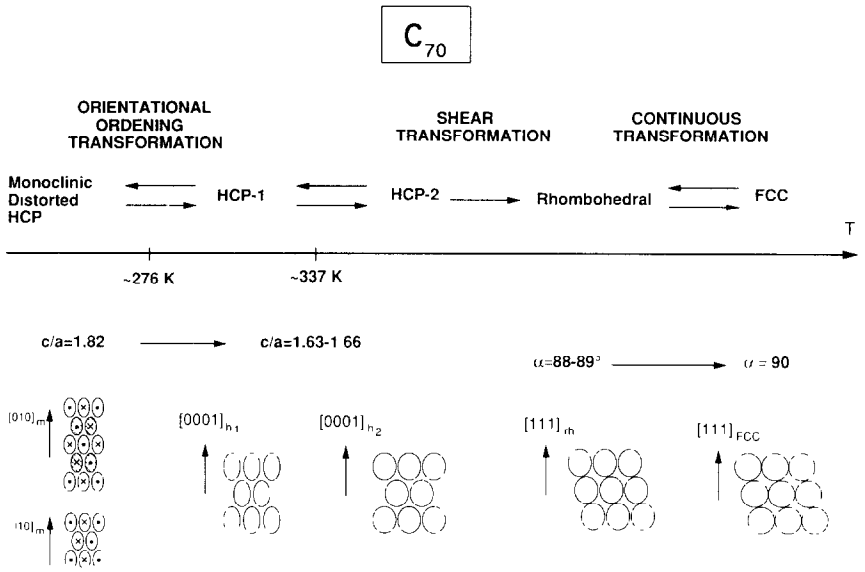

Fig. 4. Phase diagram showing the different phases, the possible transitions and the stacking modes.

five different phases and showing the possible transitions.

Most of the crystals grown have a fcc morphology. At high temperatures these crystals indeed have the fcc structure, where the molecules in the lattice have total rotational freedom [5]. On lowering the temperature the fcc lattice slightly deformes, resulting in a rhombohedral structure. Further cooling does not introduce another phase transition. Particularly, no superstructure spots are developed at liquid nitrogen temperature. Heating the crystal causes the lattice to become fcc again.

The hcp grown crystals, however, have an ideal hcp lattice at high temperatures with a c/a ratio of 1.63. Upon heating these crystals starting from room temperature a shear transformation from the ideal hcp phase with the abab... stacking into a rhombohedral one with the abcabc... stacking occurs, resulting in a c/a ratio that is slightly above the ideal value. The shear transformation is rather sluggish, occurs over a wide temperature range and is irreversible. Heating the crystal to even higher temperatures results in a fcc structure.

When freshly grown hcp crystals are cooled a transition occurs slightly above room temperature towards the "deformed" hcp structure with an elongated c axis and shortened a and b axes. The c/a ratio is now 1.82 instead of 1.63 for ideal hcp. The new length of the a axis ($a = 10.11$ Å) is close to the intermolecular distance in C_{60} crystals and therefore also close to the centre-to-centre distance of two aligned C_{70} molecules. This strongly suggests that the structure of the deformed hcp phase is a lattice in which the fivefold axes of the different molecules are oriented along the c axis of the hexagonal lattice. The molecules can now only rotate around their long axis. The calculations we will present show that the lattice energy of this phase is indeed below that of the ideal hcp structure.

Below approximately 270 K also the latter rotation is no longer possible. Since the basic hcp lattice in which all node points are occupied by molecules has not changed appreciably, it is very likely that the superstructure built on this monoclinic lattice can only differ from the hcp structure by the orientation of the molecules occupying its node points. The low temperature structure must therefore be an orientationally ordered superstructure of the deformed hcp phase.

The ordering within the close packed layers, which must be responsible for the observed superstructure spots, can be deduced assuming the stacking princi-

ple to be the same as that found for the C_{60} molecules in the simple cubic structure [7]. According to this principle the regions of large electron density along 6–6 edges of the C cage tend to face the regions of small electron density, i.e. the centres of the pentagons or hexagons, of the adjacent molecules. We here apply this principle to C_{70} molecules within a close packed layer. The molecular cages come closest to one another along their equators. Along the equator five electron-rich regions along the 6–6 edges alternate with five electron-poor regions at the centres of the hexagonal carbon rings. The stacking corresponding to the smallest electrostatic energy is one in which electron-poor regions face electron-rich regions (indicated with a "−" and "+" sign respectively in fig. 5) to the largest possible extent. For one close packed row of molecules one finds that the energetically most favourable stacking is one in which the molecules are identically oriented. However, such an arrangement can only be achieved along one close packed direction. In order to achieve the optimum two-dimensional configuration, the molecules in two adjacent parallel rows must differ 180° (or equivalently 36°)

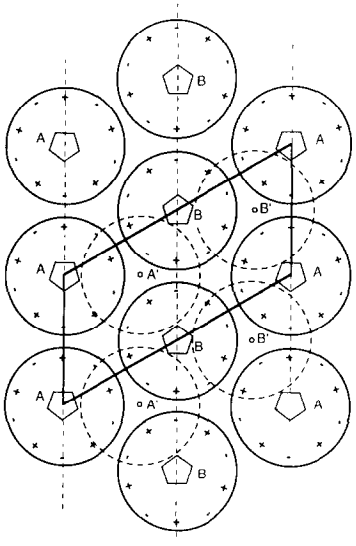

Fig. 5. Model for the stacking of orientationally ordered C_{70} molecules in the close packed planes in the monoclinic phase. A and B represent the two different orientations of molecules within a close packed layer. The molecules A′ and B′ are positioned in the next layer. Electron-rich and electron-poor regions are indicated with + and − respectively.

in orientation. It is clear from fig. 5 that then electron-rich and electron-poor regions face each other not only within one row but also to a good approximation between adjacent rows.

The stacking perpendicular to the close packed layers can now be arranged in two ways. The first possibility is an "abab..." arrangement in which the A and B rows of the different "a" planes are directly above each other, resulting in a monoclinic structure with its unique b_m axis equal to the former hexagonal c axis and an angle β close to 120°. One of the hexagonal a axes is doubled. In the X-ray diffraction measurements we found a monoclinic structure with space group $P12_1/m1$ with doubled a_h and b_h axes as compared with the hexagonal case. This result is in accord with the above described structure if we assume that the X-ray diffraction pattern was a superposition of the three different domain orientations possible for this structure.

The second possibility is an "abcdabcd..." stacking where the "c" plane is only shifted over one row with respect to the underlying "a" plane, resulting in a centered monoclinic structure with a doubled c axis ($b_m = 2c_h$). The centering is found at $\frac{1}{2}b_m + \frac{1}{2}c_m$, where $c_m = 2a_h$. This is the structure of the sample studied by TEM. Another sample was studied by X-ray diffraction and these measurements do not show spots at k=odd, but instead diffraction is found at l=odd with k=even thus violating the supposed centering condition.

We therefore suggest that both stacking modes will occur. The energy difference between the two lattices is very small as it is only due to the difference in the interactions between second nearest layers, caused by a change in relative orientation. The occurrence of two different orientational stackings, based on the same positional stacking "abab...", suggest the possibility of a new phenomenon "orientational polytypism". This new form of polytypism will clearly interfere with the extensive positional faulting observed in these crystals. The electron diffraction experiments suggest in fact that the spots due to orientational order are often streaked along c_h^* giving evidence for disorder also in the stacking of the orientationally ordered close packed layers.

6. Determination of lattice energies and morphology

6.1. The high temperature phases

To predict the morphology of the hcp and fcc C_{70} crystals grown by sublimation we have to determine the possible crystal faces and the bond strengths of both crystal structures. By means of the periodic bond chain analysis five types of faces are predicted for a hcp structure taking into account first, second and third nearest neighbour interactions, namely {1000}, {0001}, {10$\bar{1}$1}, {10$\bar{1}$2} and {11$\bar{2}$0} [8]. In case of the fcc structure three types of faces are predicted taking into account first and second nearest neighbour interactions, namely {100}, {001} and {111} [8]. To determine the stability of these faces we first have to calculate the strength of the bonds between the C_{70} molecules in both structures.

We will first consider the hcp structure. In the high temperature phase the C_{70} molecules can rotate freely around their centre of gravity. Each carbon atom can thus be considered as being smeared out over a spherical shell with a certain radius. For the 70 carbon atoms there are five different radii. Therefore the molecule can be seen as being built-up out of five spherical shells having the same centre, but different radii and different numbers of carbon atoms. For the interaction between two shells of different molecules we use an adapted form of the Lennard-Jones potential used for the interaction between two C_{60} molecules as described by Girifalco [9] who considered the atoms to be smeared out over a spherical shell. The resulting interaction potential between two C_{70} molecules is therefore a sum over 25 interactions between the five shells of both molecules,

$$\phi = -\frac{A}{48R}\sum_{i,j=1}^{5}\frac{N_iN_j}{r_ir_j}\left(\frac{1}{(r_i+r_j+R)^3}-\frac{1}{(r_i-r_j+R)^3}-\frac{1}{(-r_i+r_j+R)^3}+\frac{1}{(-r_i-r_j+R)^3}\right)+\frac{B}{360R}\sum_{i,j=1}^{5}\frac{N_iN_j}{r_ir_j}\left(\frac{1}{(r_i+r_j+R)^9}-\frac{1}{(r_i-r_j+R)^9}-\frac{1}{(-r_i+r_j+R)^9}+\frac{1}{(-r_i-r_j+R)^9}\right), \quad (1)$$

where N_i is the occupation number of shell i (i.e. the number of carbon atoms in shell i), r_i the radius of shell i and R is the distance between the centres of the two C_{70} molecules. The constants A and B can now be calculated using the given lattice parameters, the heat of sublimation for C_{70} and the assumption that the lattice energy is at minimum for the given lattice parameters. For the lattice energy the interactions up to the sixth nearest neighbour are taken into account. This energy (per mol) is equal to the heat of sublimation (43.0 ± 2.2 kcal/mol [10]). The ratio A/B is found by putting the derivative of the lattice energy with respect to R equal to zero. We thus obtain the values for A and B. The calculation was done for two cases, both for a theoretically predicted shape of the C_{70} molecule with radii (r_i) of 3.565, 3.665, 3.876, 4.029 and 4.172 Å [11] and a shape which was determined by electron diffraction with radii of 3.424, 3.690, 3.875, 3.985 and 4.097 Å [12]. The values for A and B, the bond strengths for the six different interactions and the bond lengths are given in table 1. As can be seen from this table, the two models give nearly the same bond strenghts. The bonds ϕ_1 and ϕ_2 will be dominant in the crystal structure. As was already mentioned above in the periodic bond chain analysis only ϕ_1, ϕ_2 and ϕ_3 were taken into account, which appears to be a good approximation regarding the bond strengths of ϕ_4, ϕ_5 and ϕ_6 relative to ϕ_1. (These bonds contribute less than two percent to the lattice energy.)

It has to be noted that the calculation described above was done with lattice parameters measured at room temperature. The heat of sublimation however was determined between 722 and 760 K. It is therefore interesting to do the same calculation with the lattice parameters determined at 440 K by Vaughan et al. [5]. The resulting values for A and B and the bond strengths are also given in table 1. The bond strengths appear to be in good agreement with those calculated for the room temperature lattice parameters, although the values for the fitparameter B deviate considerably.

For the calculations in the fcc structure the same method can be used as for the hcp structure. The same interaction potential is used, only some bond lengths are different. For our calculations we use the same nearest neighbour distance as in the hcp structure, i.e. 10.56 Å, which corresponds to a lattice parameter of 14.93 Å. Only three bonds appear to be important

Table 1
The definition of the six different bonds and their strengths in the ideal hcp lattice calculated in case of (I) the theoretical shape of C_{70} as predicted by Pan et al. [10], (II) the shape determined by electron diffraction [11], (III) the same shape as for (II) and lattice parameters as measured by Vaughan et al. [5]. A ($\times 10^{-78}$ J m^6) and B ($\times 10^{-135}$ J m^{12}) are the resulting fitparameters

Bond	Bond between C_{70}s at $(\frac{2}{3}, \frac{1}{3}, \frac{1}{4})$ and	Number of bonds	Bond strength ($\times 10^{-20}$ J)		
			I	II	III
ϕ_1	$(-\frac{1}{3}, \frac{1}{3}, \frac{1}{4})$	6	4.76	4.74	4.74
ϕ_2	$(\frac{1}{3}, \frac{2}{3}, \frac{3}{4})$	6	4.73	4.74	4.73
ϕ_3	$(-\frac{1}{3}, -\frac{1}{3}, \frac{3}{4})$	6	0.252	0.267	0.275
ϕ_4	$(\frac{2}{3}, \frac{1}{3}, -\frac{3}{4})$	2	0.0871	0.0919	0.0941
ϕ_5	$(-\frac{4}{3}, -\frac{2}{3}, \frac{1}{4})$	6	0.0555	0.0586	0.0610
ϕ_6	$(-\frac{5}{3}, -\frac{1}{3}, \frac{3}{4})$	12	0.0555	0.0586	0.0610
A			2.585	2.748	2.973
B			2.455	3.203	4.038

Table 2
The bond types and strenghts in the fcc lattice

Bond	Bond between C_{70}s at (0, 0, 0) and	Number of bonds	Bond strength ($\times 10^{-20}$ J)
ϕ_1	$(\frac{1}{2}, \frac{1}{2}, 0)$	12	4.74
ϕ_2	(1, 0, 0)	6	0.265
ϕ_3	$(1, \frac{1}{2}, \frac{1}{2})$	24	0.0586
ϕ_4	(1, 1, 0)	12	0.0216
ϕ_5	$(\frac{3}{2}, \frac{1}{2}, 0)$	24	0.0103

(see table 2). Using these bond strenghts it follows that within our model the lattice energy of the fcc structure is equal to that of the ideal hcp structure within a fraction of a percent. This means that there will be a very small difference in energy of these phases which explains their coexistence over a large temperature range.

6.2. The deformed hcp structure

Using the values for A and B calculated above it is also possible to calculate bond strengths for the deformed hcp phase, because A and B are considered to be independent of the crystal structure. However we assume that in this deformed phase the C_{70} molecules can merely rotate around their five fold axis and that these axes are all aligned parallel to each other along the c axis. Therefore the C_{70} molecule now has to be described as being built-up out of nine rings with smeared-out carbon atoms. The interaction potential between two C_{70} molecules is now given by a summation over 81 interactions between such rings

$$\phi = \sum_{i,j=1}^{9} \frac{N_i N_j}{4\pi^2} \int_0^{2\pi} \mathrm{d}\phi_1 \int_0^{2\pi} \mathrm{d}\phi_2 \left(\frac{-A}{x^6} + \frac{B}{x^{12}} \right), \qquad (2)$$

where

$$x^2 = [R_x - r_i \cos(\phi_1) + r_j \cos(\phi_2)]^2 + [r_i \sin(\phi_1) - r_j \sin(\phi_2)]^2 + (R_z)^2 \qquad (3)$$

and where N_i is the number of carbon atoms in ring i, r_i its radius and R_x and R_z are the distances between the centres of two rings in and perpendicular to the (a, b) plane respectively. For a hcp structure with $a = 10.11$ Å and $c = 18.57$ Å these integrals have been evaluated numerically. The resulting bond strenghts are given in table 3. The bonds ϕ_1 and ϕ_2 appear to be stronger in the deformed hcp phase than in the ideal

Table 3
The bond strengths in the deformed hcp lattice calculated for (I) the theoretically determined C_{70} shape and (II) the experimentally determined shape

Bond	Bond strength ($\times 10^{-20}$ J)	
	I	II
ϕ_1	5.84	5.94
ϕ_2	5.00	4.86
ϕ_3	0.212	0.273
ϕ_4	0.0585	0.0604
ϕ_5	0.0607	0.0735
ϕ_6	0.0607	0.0642

hcp phase. In the latter phase these bonds are of equal magnitude as is expected for an ideal hcp structure, whereas in the lower temperature phase ϕ_1 (i.e. the bond in the hexagonal plane) is clearly stronger than ϕ_2 (i.e. a bond between two molecules in adjacent hexagonal planes). The overall lattice energy is considerably higher (less negative) in the high temperature hcp phase. (-3.37×10^{-19} J/molecule for the deformed hcp lattice and -2.99×10^{-19} J/molecule for the ideal hcp lattice). The difference in lattice energies has to be larger than the difference in the entropy term in the total free energy in order to explain the phase transition. A simple calculation shows that the difference between the entropy terms of a freely rotating C_{70} molecule and of one that can merely rotate along its long axis is of the order of 0.3×10^{-19} J/molecule at room temperature, thus being smaller than the 0.38×10^{-19} J/molecule difference between the lattice energies.

A reasonable check for the validity of our calculations is to determine the axis lengths at which the lattice energy is at its minimum. This was done by calculating the lattice energy taking into account ϕ_1, ϕ_2 and ϕ_3 for different values of a and c. The axis lengths corresponding to the minimum in energy are $a=9.9$ Å and $c=18.4$ Å, which is in good agreement (within 2%) with the experimentally determined values.

6.3. The theoretical morphology

The following method to find the equilibrium crystal habit is to a large extent the same as the one we used for C_{60} crystals [6]. Using the bond strengths we are able to calculate the roughening temperatures of the predicted faces by means of a statistical mechanical Ising model [13,14]. The resulting values are given in table 4 for both the fcc and (ideal) hcp structure. Considering the rule of thumb that the calculated Ising temperatures are typically about 10% less than the actual roughening temperatures we find that the {110} face will be roughened for both crystal structures at the growth temperature of the crystals. However, the growth temperature is close to the roughening temperature of the hcp $\{10\bar{1}2\}$ face resulting in a decreased stability and a higher growth velocity of this face. Therefore it is very likely that this face will not occur on the growth form. The hcp crystal morphology will thus be determined by three different types of faces, while that of the fcc crystal will show merely two types of faces.

Table 4
Theoretical roughening temperatures for the crystal faces of hcp and fcc C_{70}. Note that we use a growth temperature of approximately 925 K

Face	T_R (hcp) (K)	T_R (fcc) (K)
{111}	–	3.1×10^3
{100}	3.2×10^3	2.0×10^3
{001}	3.2×10^3	–
{101}	2.6×10^3	–
{102}	1.0×10^3	–
{110}	0.67×10^3	0.66×10^3

A measure for the morphological importance of a face is the specific surface free energy, which can be approximated by taking $E_{att}d_{hkl}$, where E_{att} is the attachment energy, which is the sum of the energies of the bonds per molecule which lack due to a surface and d_{hkl} is the distance between two adjacent layers $\{hkl\}$. The equilibrium crystal form can now be obtained using the Gibbs–Wulff construction. In fig. 6a

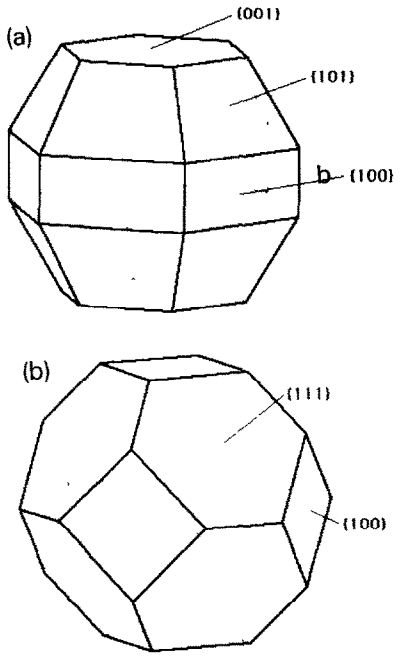

Fig. 6. Theoretical morphology of C_{70} crystals having (a) a hcp structure and (b) a fcc structure.

the resulting morphology for the hcp crystal is given in case the $\{10\bar{1}2\}$ face is roughened. All the remaining three types of faces appear on the crystal. For the fcc crystal the morphology is given in fig. 6b. When the predicted morphologies are compared with the observed crystal shapes we can conclude that the theoretical equilibrium forms describe the actual shapes quite well. Only the presence of the hcp $\{100\}$ faces could not be verified.

7. Conclusion

We have succeeded in growing C_{70} crystals from the vapour phase. By means of X-ray diffraction and TEM the different phases occurring in these crystals have been determined.

Most C_{70} crystals grow in the fcc structure, while a small fraction forms a hcp phase. The morphology of both the hcp and the fcc grown crystals is in agreement with the growth forms predicted using the calculated bond energies, although the fcc crystals were severely twinned and the hcp crystals were never completely developed.

The hcp phase is more stable at low temperatures than the fcc structure due to a higher lattice energy, the energy difference being very small, however. Thus, the fact that also at the temperature at which the crystals are grown hcp crystals are formed can be understood. The phase transition hcp → fcc is irreversible. On lowering the temperature of the fcc grown crystals a rhombohedral distortion is encountered.

The fcc grown crystals studied under the TEM turned out to be severely faulted. Due to the small difference in lattice energy of the two types of close packed lattices stacking faults can easily be introduced. The fact that X-ray diffraction measurements did not show a well defined lattice of Bragg reflections also indicates the presence of many defects. The structure of the ideal hcp grown crystals for that matter was better defined. The space group of this phase is expected to be $P6_3/mmc$ ($c/a=1.63$). On lowering the temperature the ideal hcp crystals transform into a deformed hcp phase ($P6_3/mmc$ ($c/a=1.82$)) slightly above room temperature, where the initially free rotations of the molecules are frozen-in to a mere free rotation around their long axis, which is oriented parallel to the six-fold axis of the hcp lattice. The lattice energy of this phase is considerably lower than that of the ideal hcp structure. We assume this phase transition to be the one Vaughan reported on at 337 K [5]. Recent Raman measurements [15] observe this transition at approximately 323 K. A final phase transition occurs at approximately 270 K (Vaughan et al. reported on a phase transition with an onset at 276 K) for which the free rotation around the c axis is also frozen-in. The resulting phase is monoclinic having its unique axis equal to the former hexagonal c axis and an angle β close or equal to 120°. One of the hexagonal a axes is doubled. The former hexagonal plane now consists of two alternating rows of fixed C_{70} molecules, the molecules being oriented parallel to each other within the rows and antiparallel with respect to the neighbouring rows. The stacking perpendicular to this plane can be arranged in two ways, one resulting in $b_m=c_h$, the other one in $b_m=2c_h$ and a centered b_m face. Both stacking modes will occur, the energy difference between the two lattices being very small as it is only due to the difference in the interactions between second nearest layers, caused by a change in relative orientation of the molecules.

Acknowledgement

We gratefully acknowledge the financial support of the Netherlands Organization for Scientific Research (NWO/SON) and the Dutch Foundation for Fundamental Research of Matter (FOM). Part of this work has been made possible with the financial help of the National Fund for Scientific Research (Belgium) and of the Services for Science Policy (IUAP 11) of the Belgian Government.

References

[1] W. Krätschmer, L.D. Lamb, K. Fostiropoulos and D.R. Huffman, Nature 347 (1990) 354.

[2] P.A. Heiney, J.E. Fischer, A.R. McGhie, W.J. Romanov, A.M. Denenstein, J.P. McCauley Jr., A.B. Smith III and D.E. Cox, Phys. Rev. Letters 66 (1991) 2911.

[3] R. Sachidanandam and A.B. Harris, Phys. Rev. Letters 67 (1991) 1467.

[4] G. van Tendeloo, S. Amelinckx, M.A. Verheijen, P.H.M. van Loosdrecht and G. Meijer, Phys. Rev. Letters (1992), in press.

[5] G.B.M. Vaughan, P.A. Heiney, J.E. Fischer, D.E. Luzzi, D.A. Ricketts-Foot, A.R. McGhie, W.J. Romanow, B.H. Allen, N. Coustel, J.P. McCauley Jr. and A.B. Smith III, Science 254 (1991) 1350.
[6] M.A. Verheijen, H. Meekes, G. Meijer, E. Raas and P. Bennema, Chem. Phys. Letters 191 (1992) 339.
[7] W.I.F. David, R.M. Ibberson, J.C. Matthewman, K. Prassides, T.J.S. Dennis, J.P. Hare, H.W. Kroto, R. Taylor and D.R.M. Walton, Nature 353 (1991) 147.
[8] Hartman, Ph. D. Thesis, University of Groningen (Excelsior, The Hague, 1953).
[9] L.A. Girifalco, J. Phys. Chem. 96 (1992) 858.
[10] C. Pan, M.P. Sampson, Y. Chai, R.H. Hauge and J.L. Margrave, J. Phys. Chem. 95 (1991) 2944.
[11] J. Baker, P.W. Fowler, P. Lazzeretti, M. Malagoli and R. Zanasi, Chem. Phys. Letters 184 (1991) 182.
[12] D.R. McKenzie, C.A. Davis, D.J.H. Cockayne, D.A. Muller and A.M. Vassallo, Nature 355 (1992) 622.
[13] J.J.M. Rijpkema, H.J.F. Knops, P. Bennema and J.P. van der Eerden, J. Cryst. Growth 61 (1982) 295.
[14] P. Bennema, in: Sir Charles Frank, an eightieth birthday tribute, eds. R.G. Chambers, J.E. Enderby, A. Keller, A.R. Lang and J.W. Steeds, (Hilger, Bristol, 1991) p. 46.
[15] P. van Loosdrecht, to be published.